

# Single-photon router based on a modulated cavity optomechanical system

Jun-Hao Liu, Ya-Fei Yu,\* and Zhi-Ming Zhang†

Guangdong Provincial Key Laboratory of Nanophotonic Functional Materials & Devices (SIPSE),  
and Guangdong Provincial Key Laboratory of Quantum Engineering & Quantum Materials,  
South China Normal University, Guangzhou 510006, China

We investigate the routing of a single-photon in a modulated cavity optomechanical system, in which the cavity is driven by a strong coupling field, the mechanical resonator (MR) is modulated by a weak coherent field, and the signal photon is made up of a sequence of pulses with exactly one photon per pulse. We demonstrate that, when there is no weak coherent field modulating the MR, the system cannot act as a single-photon router, since the signal will be completely covered by the quantum and thermal noises. With the existence of the weak coherent field, we can achieve the routing of the single-photon by changing the frequency of the weak coherent field, and the system can be immune to the quantum noises and thermal noises when the MR is cooled to its quantum ground state.

PACS numbers:

## I. INTRODUCTION

It is known that quantum network is an important ingredient for transmitting information in quantum communication. In the building of quantum network, quantum router is an essential element since it can coherently control the propagation path of the quantum signals. In the past few decades, scientists have demonstrated that many physical effects and physical systems, such as quantum interference [1], electromagnetically induced transparency [2], coupled waveguide array [3–5], can be used to realize the routing of the photons. Recently, many theoretical and experimental researches aiming at achieving the quantum router in the single-photon level have been reported [6–10]. Hall et al. demonstrated the routing of single-photon without disturbing the photons' quantum state with the help of strong cross-phase modulation [11]. Hoi et al. achieved a single-photon router in the microwave regime by using a superconducting transmon qubit [12]. Zhou et al. proposed an experimentally accessible single-photon routing scheme using a type three-level atom embedded in a coupled-resonator waveguide [13].

We also notice that the realization of a single-photon router has been researched in cavity optomechanical system. In Ref [14], the authors have shown how nanomechanical mirrors (NMMs) in optical cavity can be used to build single-photon routers. However, their analysis is inadequate. We find that, their scheme actually cannot achieve the routing of a single-photon, since the signal will be completely covered by the quantum and thermal noises. In this paper, we propose a scheme based on a modulated cavity optomechanical system to realize the single-photon router. In our system, the cavity is driven by a strong coupling field, and the mechanical resonator

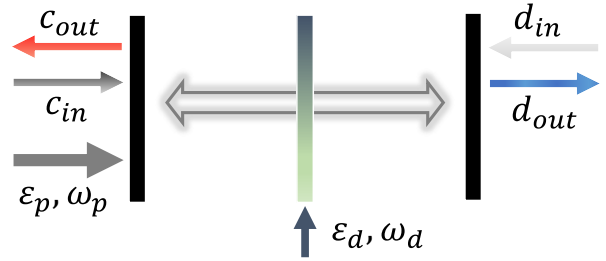


FIG. 1: (color online) Schematic diagram of our proposed model. A mechanical resonator (MR) of partial reflection is inserted between two fixed mirrors. A strong coupling field is injected from the left. The MR is modulated by a weak coherent field.

(MR) is modulated by a weak coherent field. We can achieve the routing of the single-photon by changing the frequency of the weak coherent field. Moreover, our system can be immune to the quantum noises and thermal noises when the MR is cooled to its quantum ground state.

This paper is organized as follows. In Section II we introduce the theoretical model. In Section III, we consider the case of that there is no weak coherent field modulating the MR. We show and explain why in this case, the system cannot act as a single-photon router. Next in Section IV, we consider the case of that MR is modulated by a weak coherent field. We exhibit how does the single-photon router work in our scheme, and discuss the effects of the quantum and thermal noises on this single-photon router. Finally in Section V, we provide a brief summary.

## II. MODEL

Our proposed scheme is shown in Fig. 1. we consider a cavity optomechanical system with a mechanical resonator (MR) of partial reflection inserted between two

\*Electronic address: yuyafei@m.scnu.edu.cn

†Electronic address: zhangzhiming@m.scnu.edu.cn

fixed mirrors. The cavity is driven by a strong coupling field  $\varepsilon_p = \sqrt{2P\kappa}/(\hbar\omega_p)$  with frequency  $\omega_p$ . The MR is modulated by a weak coherent field with amplitude  $\varepsilon_d$  and frequency  $\omega_d$ , this modulation can be realized by, e.g., parametrically modulating the spring constant of the MR at twice that MR's resonance frequency [15, 16]. The Hamiltonian of the system in the rotating frame at the frequency  $\omega_p$  of the coupling field is given by ( $\hbar = 1$ )

$$H = \Delta\hat{a}^\dagger\hat{a} + g_0\hat{a}^\dagger\hat{a}(\hat{b}^\dagger + \hat{b}) + i\varepsilon_p(\hat{a}^\dagger - \hat{a}) + \omega_m\hat{b}^\dagger\hat{b} + i\varepsilon_d[(\hat{b}^\dagger)^2e^{-i2\omega_d t} - (\hat{b})^2e^{i2\omega_d t}], \quad (1)$$

where  $\Delta = \omega_c - \omega_p$  is the frequency detuning between the cavity field and the coupling field.  $\hat{a}$  and  $\hat{b}$  are the annihilation operators of the cavity mode and the mechanical mode with frequency  $\omega_c$  and  $\omega_m$ , respectively,  $g_0$  is the single-photon optomechanical coupling strength between the cavity field mode and the mechanical mode.

The system dynamics is fully described by the set of the quantum Langevin equations (QLEs)

$$\frac{d\hat{a}}{dt} = -(2\kappa + i\Delta)\hat{a} - ig_0\hat{a}(\hat{b}^\dagger + \hat{b}) + \varepsilon_p + \sqrt{2\kappa}\hat{c}_{in} + \sqrt{2\kappa}\hat{d}_{in}, \quad (2)$$

$$\frac{d\hat{b}}{dt} = -(\gamma + i\omega_m)\hat{b} - ig_0\hat{a}^\dagger\hat{a} + 2\varepsilon_d e^{-i2\omega_d t}\hat{b}^\dagger + \sqrt{2\gamma}\hat{b}_{in}, \quad (3)$$

where  $2\kappa$  is the total damping rate of the cavity. The input field  $\hat{c}_{in}$  is in a single-photon Fock state, the correlation functions are  $\langle \hat{c}_{in}^\dagger(\Omega)\hat{c}_{in}(\omega) \rangle = S_{in}(\omega)\delta(\omega + \Omega)$ ,  $\langle \hat{c}_{in}(\Omega)\hat{c}_{in}^\dagger(\omega) \rangle = [S_{in}(\Omega) + 1]\delta(\omega + \Omega)$ . It should be point out that, when we use such a single-photon state as the input state to a cavity, we should assume that its center frequency is resonant with the cavity [17, 18]. Its spectrum is given by  $S_{in}(\omega) = \frac{\Gamma/\pi}{(\omega - \omega_c)^2 + \Gamma^2}$ , in which  $\Gamma$  is the decay rate of the single photon. The incoming vacuum field  $\hat{d}_{in}$  is characterized by  $\langle \hat{d}_{in}(\Omega)\hat{d}_{in}^\dagger(\omega) \rangle = \delta(\Omega + \omega)$ . The mechanical mode has the damping rate  $\gamma$  with the mechanical input operator  $\hat{b}_{in}$  satisfying  $\langle \hat{b}_{in}^\dagger(\Omega)\hat{b}_{in}(\omega) \rangle = n_{th}\delta(\Omega + \omega)$ ,  $\langle \hat{b}_{in}(\Omega)\hat{b}_{in}^\dagger(\omega) \rangle = (n_{th} + 1)\delta(\Omega + \omega)$  in the frequency domain, where  $n_{th}$  is the thermal phonon occupation number at a finite temperature.

We assume that the cavity field is driving by a strong coupling field  $\varepsilon_p$  and the MR is modulated by a weak coherent field  $\varepsilon_d$ , then we can make a transformations  $\hat{a} \rightarrow \alpha + \delta\hat{a}$ , and  $\hat{b} \rightarrow \beta + \delta\hat{b}$ , where  $\alpha(\beta)$  and  $\delta\hat{a}(\delta\hat{b})$  are the steady state mean value and quantum fluctuation of the cavity mode (mechanical mode), respectively. Substituting the division forms into the QLEs (2)-(3), and setting all the time derivations at the steady parts to be

zero, and we can obtain

$$\alpha = \frac{\varepsilon_p}{2\kappa + i\Delta + ig_0(\beta + \beta^*)}, \quad (4)$$

$$\beta = \frac{-ig_0|\alpha|^2}{\gamma + i\omega_m}. \quad (5)$$

In this paper, we consider that our system works near the red sideband  $\Delta = \omega_m$ . For simplicity, we rewrite  $\delta\hat{a}(\delta\hat{b})$  as  $\hat{a}(\hat{b})$  in the following sections.

### III. WITHOUT THE WEAK COHERENT FIELD

In this section, we consider the case of that there is no a weak coherent field modulating the MR. We should point out that, this situation has been discussed in Ref [14]. However, their analysis is inadequate and the conclusion is incorrect, so we make a recalculation and a rediscussion. When  $\varepsilon_d = 0$ , the linearized Hamiltonian of the system can be expressed as

$$H_I = \Delta'\hat{a}^\dagger\hat{a} + \omega_m\hat{b}^\dagger\hat{b} + G(\hat{a}^\dagger\hat{b} + \hat{a}\hat{b}^\dagger) + G^*(\hat{a}\hat{b}^\dagger + \hat{a}^\dagger\hat{b}), \quad (6)$$

where  $G = g_0\alpha$ ,  $\Delta' = \Delta + g_0(\beta + \beta^*) \simeq \Delta$ .

We define a vector  $v(t) = (\hat{a}(t), \hat{b}(t), \hat{a}^\dagger(t), \hat{b}^\dagger(t))^T$  in terms of the operators of the system modes. By substituting  $v(t)$  and  $H_I$  into the quantum Langevin equation, we can obtain

$$\frac{dv(t)}{dt} = Mv(t) + \sqrt{2\kappa}v_{c,in} + \sqrt{2\kappa}v_{d,in} + \sqrt{2\gamma}v_{b,in}, \quad (7)$$

where  $v_{x,in} = (\hat{x}_{in}(t), 0, \hat{x}_{in}^\dagger(t), 0)^T$  ( $x = c, d$ ),  $v_{b,in} = (0, \hat{b}_{in}(t), 0, \hat{b}_{in}^\dagger(t))^T$ , and

$$M = \begin{pmatrix} -2\kappa - i\Delta & -iG & 0 & -iG \\ -iG^* & -\gamma - i\Delta_m & -iG & 0 \\ 0 & iG^* & i\Delta - 2\kappa & iG^* \\ iG^* & 0 & iG & i\Delta_m - \gamma \end{pmatrix}, \quad (8)$$

the system is stable only if the real parts of all the eigenvalues of matrix  $M$  are negative. The stability conditions can be explicitly given by using the Routh-Hurwitz criterion [19–21], and the stability conditions are fulfilled in the system with our used parameters. Moreover, without loss of generality, we take  $G$  as a real number in the following calculation.

In experiments, fluctuations of the electromagnetic field are more convenient to measure in the frequency domain than in the time domain. Therefore, we introduce the Fourier transform of the operators

$$\hat{o}(\omega) = \int_{-\infty}^{+\infty} \hat{o}(t)e^{i\omega t} dt, \quad (9)$$

$$\hat{o}^\dagger(\omega) = \int_{-\infty}^{+\infty} \hat{o}^\dagger(t)e^{i\omega t} dt, \quad (10)$$

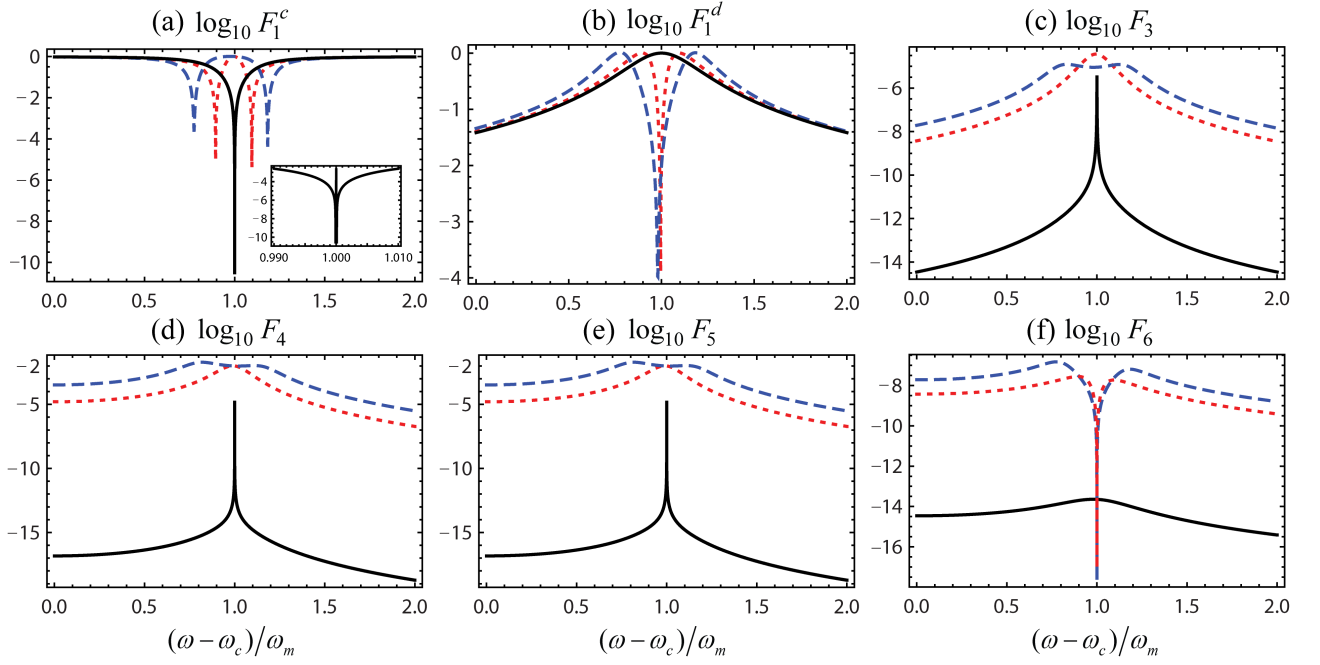


FIG. 2: (color online) The spectrums of the scattering probabilities  $F_1^c$ ,  $F_1^d$ ,  $F_3$ ,  $\dots$ ,  $F_6$  for  $G/\omega_m = 10^{-4}$  (black solid lines),  $G/\omega_m = 0.1$  (red dotted lines),  $G/\omega_m = 0.2$  (blue dashed lines). The other parameters are stated in the text.

where  $\hat{o} = \hat{a}$ ,  $\hat{b}$ , then we can solve the linearized QLEs (7) in the frequency domain

$$v(\omega) = -(M + i\omega I)^{-1} [\sqrt{2\kappa}v_{c,in}(\omega) + \sqrt{2\kappa}v_{d,in}(\omega) + \sqrt{2\gamma}v_{b,in}(\omega)], \quad (11)$$

where  $v(\omega) = (\hat{a}(\omega), \hat{b}(\omega), \hat{a}^\dagger(\omega), \hat{b}^\dagger(\omega))^T$ ,  $v_{x,in}(\omega) = (\hat{x}_{in}(\omega), 0, \hat{x}_{in}^\dagger(\omega), 0)^T$  ( $x = c, d$ ), and  $v_{b,in}(\omega) = (0, \hat{b}_{in}(\omega), 0, \hat{b}_{in}^\dagger(\omega))^T$ , then we can obtain

$$\hat{a}(\omega) = f(\omega)v_{in}(\omega), \quad (12)$$

where  $f(\omega) = (f_1(\omega), f_2(\omega), f_3(\omega), f_4(\omega), f_5(\omega), f_6(\omega))$ , and  $v_{in}(\omega) = (\hat{c}_{in}(\omega), \hat{d}_{in}(\omega), \hat{b}_{in}(\omega), \hat{c}_{in}^\dagger(\omega), \hat{d}_{in}^\dagger(\omega), \hat{b}_{in}^\dagger(\omega))^T$ , the concrete forms of the coefficients  $f_1(\omega), \dots, f_6(\omega)$  are tediously long, we will not write out here.

The relation among the input, internal, and output fields is given as [22]

$$\hat{x}_{out}(\omega) = -\hat{x}_{in}(\omega) + \sqrt{2\kappa}\hat{a}(\omega), \quad x = c, d, \quad (13)$$

then we can write the operators of the output fields as

$$\hat{c}_{out}(\omega) = f^c(\omega)v_{in}(\omega), \quad \hat{d}_{out}(\omega) = f^d(\omega)v_{in}(\omega), \quad (14)$$

where  $f^c(\omega) = (f_1^c(\omega) - 1, f_2^c(\omega), f_3^c(\omega), f_4^c(\omega), f_5^c(\omega), f_6^c(\omega))$ ,  $f^d(\omega) = (f_1^d(\omega), f_2^d(\omega) - 1, f_3^d(\omega), f_4^d(\omega), f_5^d(\omega), f_6^d(\omega))$ , and  $f_j^c(\omega) \equiv \sqrt{2\kappa}f_j(\omega)$  ( $j = 1, 2, 3, 4, 5, 6$ ).

The spectrums of the output fields are defined by

$$S_{x,out}(\omega) = \int d\Omega \langle \hat{x}_{out}^\dagger(\Omega)\hat{x}_{out}(\omega) \rangle, \quad x = c, d. \quad (15)$$

By substituting the expressions of  $\hat{c}_{out}(\omega)$  and  $\hat{d}_{out}(\omega)$  into Eq. (15), and using the correlation functions, one can obtain

$$S_{c,out}^I(\omega) = F_1^c S_{in}(\omega) + F_4 S_{vac}(-\omega) + F_5 + F_3 n_{th} + F_6 (n_{th} + 1), \quad (16)$$

$$S_{d,out}^I(\omega) = F_1^d S_{in}(\omega) + F_4 S_{vac}(-\omega) + F_5 + F_3 n_{th} + F_6 (n_{th} + 1), \quad (17)$$

where  $F_1^c = |f_1^c(\omega) - 1|^2$ ,  $F_1^d = |f_1^d(\omega)|^2$ ,  $S_{vac}(-\omega) = S_{in}(-\omega) + 1$ ,  $F_j = |f_j^c(\omega)|^2$  ( $j = 3, 4, 5, 6$ ).

We can see that, the spectrum of the output fields  $S_{c,out}^I(\omega)$  and  $S_{d,out}^I(\omega)$  both contain five components. For  $S_{c,out}^I(\omega)$ ,  $F_1^c$  represents the scattering probability of the input field  $\hat{c}_{in}(\omega)$ .  $F_4$  denotes the scattering probability of the fluctuation of the input field  $\hat{c}_{in}(\omega)$ .  $F_5$  is the scattering probability of the fluctuation of the vacuum field  $\hat{d}_{in}(\omega)$ .  $F_3$  and  $F_6$  denote the scattering probability of the input mechanical noise and its fluctuation, respectively. Furthermore, we find that even if there is no input signal photon, the output fields will also be generated by the vacuum fluctuation and thermal noise. For a good single photon router, it should not be influenced by these quantum and thermal noises.

In this paper, the parameter we used are the same as that in Ref [14]: the wavelength of the coupling field  $\lambda = 1054$  nm,  $L = 6.7$  cm,  $m = 40$  ng,  $\omega_m = 2\pi \times 134$  kHz,  $\gamma_m = 0.76$  Hz,  $\kappa = 0.1\omega_m$ .

Next we numerically evaluate the reflection spectrum  $F_1^c$  and the transmission spectrum  $F_1^d$  for different effective optomechanical coupling strength  $G$ , the results are

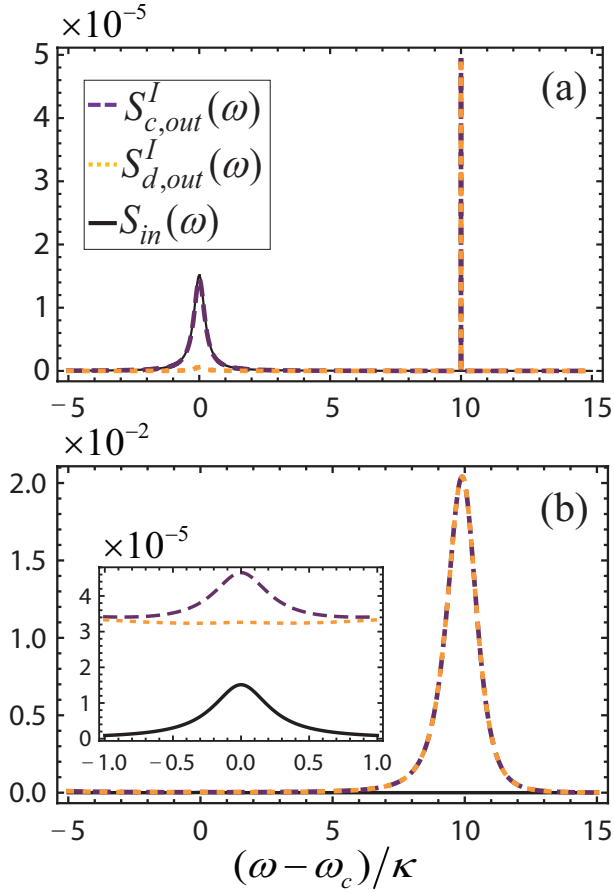


FIG. 3: (color online) The spectrum of the output fields  $S_{c,out}^{mw}(\omega)$  (purple dashed lines),  $S_{d,out}^{nw}(\omega)$  (orange dotted lines) and the input fields  $S_{in}(\omega)$  (black solid lines) for different  $G$ : (a)  $G/\omega_m = 10^{-4}$ , (b)  $G/\omega_m = 0.1$ . The thermal phonon occupation number  $n_{th} = 0$ , and the other parameters are the same as in Fig. 2.

shown in Fig. 2(a) and Fig. 2(b). It can be seen that, when  $G$  is very small (we notice that in Ref [14], they consider the situation by making the power of the coupling field  $P = 0$ . However, the linearization demands  $P \neq 0$ , and  $G \gg g_0$ , so here we let  $G = 10^{-4}\omega_m \gg g_0$ ), the spectrum of the transmitted single-photon will exhibit a peak, while the spectrum of the reflected single-photon will exhibit a valley at  $\omega - \omega_c = \omega_m$ , and we have  $F_1^c \approx 0$  and  $F_1^d \approx 1$ , now the single-photon will be completely transmitted through the cavity to the right output port. With the increase of  $G$ ,  $F_1^d$  and  $F_1^c$  will exhibit a dip and a rise at  $\omega - \omega_c = \omega_m$ , respectively. When  $G = 0.1\omega_m$  or  $0.2\omega_m$ , we have  $F_1^c \approx 1$ , and  $F_1^d \approx 0$ , now the single-photon will be completely reflected through the cavity to the left output port. Furthermore, now the spectrums will exhibit a split at  $\omega - \omega_c = \omega_m \pm G$ , and this is associated with the normal mode splitting [23, 24].

Now we consider the effects of the quantum and thermal noises. In Fig. 2(c)-(f), we plot the spectrums of the scattering probabilities  $F_3, \dots, F_6$ , respectively. We find

that, at  $\omega - \omega_c = \omega_m, F_3, \dots, F_6$  have the following order of magnitudes: when  $G = 10^{-4}\omega_m$ ,  $F_3 \sim 10^{-6}$ ,  $F_4, F_5 \sim 10^{-5}$ , and  $F_6 \sim 10^{-14}$ , when  $G = 0.1\omega_m$  or  $0.2\omega_m$ ,  $F_3 \sim 10^{-5}$ ,  $F_4, F_5 \sim 10^{-2}$ , and  $F_6 \sim 10^{-17}$ . I.e., with the increase of  $G$ , the vacuum fluctuations of the input fields  $\hat{c}_{in}(\omega)$  and  $\hat{d}_{in}(\omega)$  have been strongly amplified, while the vacuum fluctuation of the input field  $\hat{b}_{in}(\omega)$  has been effectively suppressed.

Moreover, we should also give the order of magnitude of the signal. We consider the single-photon has a narrower linewidth than the cavity ( $\Gamma = 0.25\kappa$ ), the spectrum of the single-photon has the peak value  $S_{in}(\omega_c) \sim 10^{-5}$ . However, now the operating frequency of the system is at  $\omega - \omega_c = \omega_m$ , the signal  $S_{in}(\omega_c + \omega_m)$  has order of magnitude  $10^{-8}$ . By comparing these order of magnitudes, we can easily find that,  $F_1^c S_{in}(\omega_c + \omega_m)$  or  $F_1^d S_{in}(\omega_c + \omega_m)$  is far less than  $F_4 + F_5 + F_3 n_{th} + F_6 n_{th}$  whether when  $G = 10^{-4}\omega_m$  or  $G = 0.1\omega_m, 0.2\omega_m$ , i.e., the signal will be completely covered by the quantum and thermal noises.

To further illustrate our point, we present the spectrums of the output fields  $S_{c,out}^I(\omega)$  and  $S_{d,out}^I(\omega)$  for  $G = 10^{-4}\omega_m$  and  $G = 0.1\omega_m$  in Fig. 3(a) and Fig. 3(b), respectively. We also plot the spectrum of the input field  $S_{in}(\omega)$  as a comparison. It can be seen that in Fig. 3(a):  $S_{c,out}^I(\omega)$  and  $S_{d,out}^I(\omega)$  both exhibit a very narrow peak at  $\omega - \omega_c = \omega_m$ , and we have  $S_{c,out}^I(\omega_c + \omega_m) \approx S_{d,out}^I(\omega_c + \omega_m) \sim 10^{-5}$ ; at  $\omega - \omega_c = 0$ ,  $S_{c,out}^I(\omega)$  and  $S_{in}(\omega)$  are almost coincide ( $S_{c,out}^I(\omega_c) \approx S_{in}(\omega_c) \sim 10^{-5}$ ), and  $S_{d,out}^I(\omega_c) \approx 0$ . We can see that in Fig. 3(b):  $S_{c,out}^I(\omega)$  and  $S_{d,out}^I(\omega)$  both exhibit a wide peak at  $\omega - \omega_c = \omega_m$ , and we have  $S_{c,out}^I(\omega_c + \omega_m) \approx S_{d,out}^I(\omega_c + \omega_m) \sim 10^{-2}$ ; at  $\omega - \omega_c = 0$ , we have  $S_{c,out}^I(\omega_c) > S_{d,out}^I(\omega_c) > S_{in}(\omega_c)$ . All of the above phenomena can be easily explained by viewing Fig. 2 (note that we have assumed that the thermal phonon occupation number  $n_{th} = 0$  in Fig. 3). According to the above analyzes, we can conclude that, in this case, this system cannot act as a single-photon router.

#### IV. WITH THE WEAK COHERENT FIELD

In this section, we consider the case of that there is a weak coherent field modulating the MR. In the rotation frame transformation with  $H' = \omega_d(\hat{a}^\dagger \hat{a} + \hat{b}^\dagger \hat{b})$ , the linearized Hamiltonian of the system can be expressed as

$$H_{II} = \delta \hat{a}^\dagger \hat{a} + \Delta_m \hat{b}^\dagger \hat{b} + G(\hat{a}^\dagger \hat{b} + \hat{a} \hat{b}^\dagger) + i\varepsilon_d[(\hat{b}^\dagger)^2 - (\hat{b})^2], \quad (18)$$

where  $\delta = \Delta - \omega_d$ , and  $\Delta_m = \omega_m - \omega_d$ . In addition, using the rotating-wave approximation, we have omitted the high-frequency oscillation terms  $\hat{a}^\dagger \hat{b}^\dagger e^{i2\omega_d t}$  and  $\hat{a} \hat{b} e^{-i2\omega_d t}$ .

By substituting  $v(t)$  and  $H_{II}$  into the quantum Langevin equation, we can obtain

$$\frac{dv(t)}{dt} = M'v(t) + \sqrt{2\kappa}v_{c,in} + \sqrt{2\kappa}v_{d,in} + \sqrt{2\gamma}v_{b,in}, \quad (19)$$

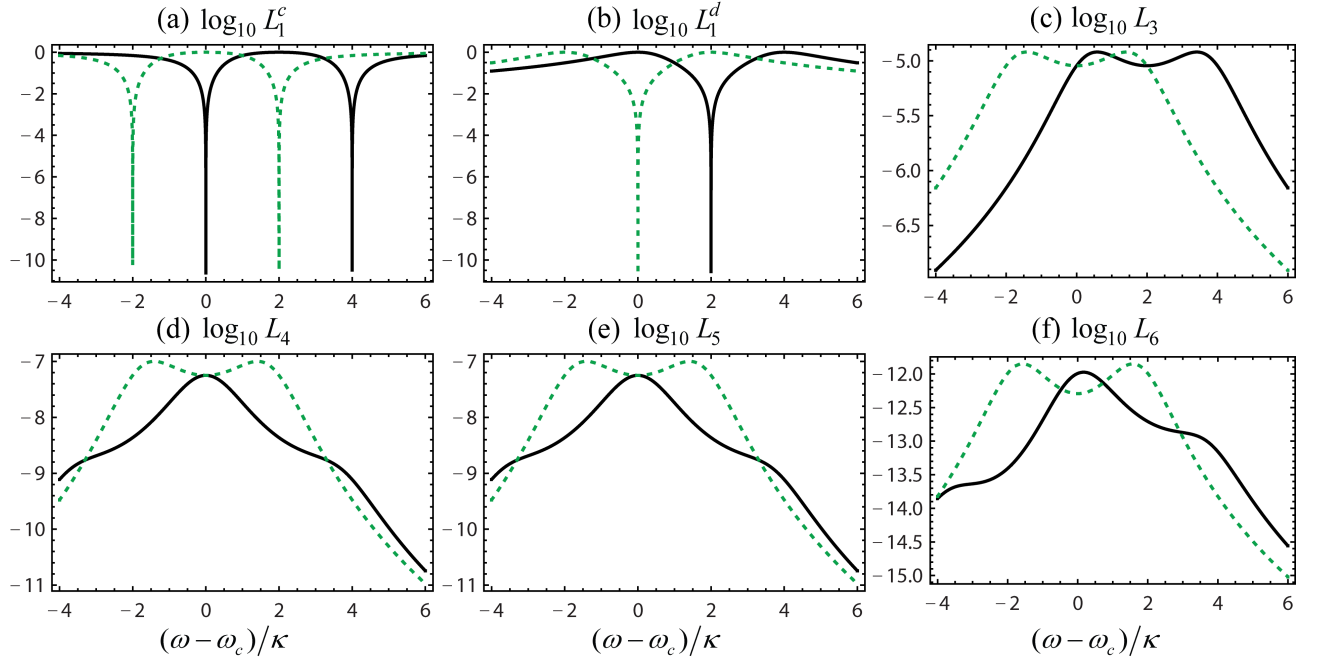


FIG. 4: (color online) The spectrums of the scattering probabilities  $L_1^c$ ,  $L_1^d$ ,  $L_3$ ,  $\dots$ ,  $L_6$  for  $\omega_d/\omega_m = 0.8$  (black solid lines),  $\omega_d/\omega_m = 1$  (green dotted lines). The amplitude of the weak coherent field  $\varepsilon_d/\omega_m = 2.56 \times 10^{-5}$ , and the other parameters are stated in the text.

and

$$M' = \begin{pmatrix} -2\kappa - i\delta & -iG & 0 & 0 \\ -iG & -\gamma - i\Delta_m & 0 & 2\varepsilon_d \\ 0 & 0 & i\delta - 2\kappa & iG \\ 0 & 2\varepsilon_d & iG & i\Delta_m - \gamma \end{pmatrix}, \quad (20)$$

the stability conditions of the matrix  $M'$  has also been verified by using the Routh-Hurwitz criterion with our used parameters. Because the next calculations are similar with that in section III, we will directly give the final results, the spectrums of the output fields are obtained as

$$S_{c,out}^{II}(\omega) = L_1^c S_{in}(\omega) + L_4 S_{vac}(-\omega) + L_5 + L_3 n_{th} + L_6 (n_{th} + 1), \quad (21)$$

$$S_{d,out}^{II}(\omega) = L_1^d S_{in}(\omega) + L_4 S_{vac}(-\omega) + L_5 + L_3 n_{th} + L_6 (n_{th} + 1), \quad (22)$$

in which  $L_1^c$ ,  $L_1^d$ ,  $L_4$ ,  $\dots$ ,  $L_6$  have the same physical significance with  $F_1^c$ ,  $F_1^d$ ,  $F_4$ ,  $\dots$ ,  $F_6$ , respectively. The concrete forms of  $L_1^c$ ,  $L_1^d$ ,  $L_4$ ,  $\dots$ ,  $L_6$  are too verbose to be given.

Now we show how does the single-photon router work in our scheme. In our system, with the existence of the weak coherent field, the effective frequency of the mechanical mode becomes  $\Delta_m = \omega_m - \omega_d$ . Furthermore, we choose  $G = 0.2\omega_m = 2\kappa$ , and the transmission spectrum  $L_1^d$  and the reflection spectrum  $L_1^c$  will exhibit a split. So we can see that in Fig. 3(a) and Fig. 3(b), when  $\omega_d = 0.8\omega_m$  ( $\Delta_m = 2\kappa$ ),  $L_1^c$  exhibit a peak at  $\omega - \omega_c = \Delta_m$

and a valley at  $\omega - \omega_c = \Delta_m \pm G$ ,  $L_1^d$  exhibit a valley at  $\omega - \omega_c = \Delta_m$  and a peak  $\omega - \omega_c = \Delta_m \pm G$ . The above features will result that, at  $\omega - \omega_c = 0$ ,  $L_1^c \approx 0$  and  $L_1^d \approx 1$ , now the single-photon will be completely transmitted through the cavity to the right output port. With the increase of  $\omega_d$ , the curves integrally move to the left, when  $\omega_d = \omega_m$  ( $\Delta_m = 0$ ), we have  $L_1^c \approx 1$  and  $L_1^d \approx 0$  at  $\omega - \omega_c$

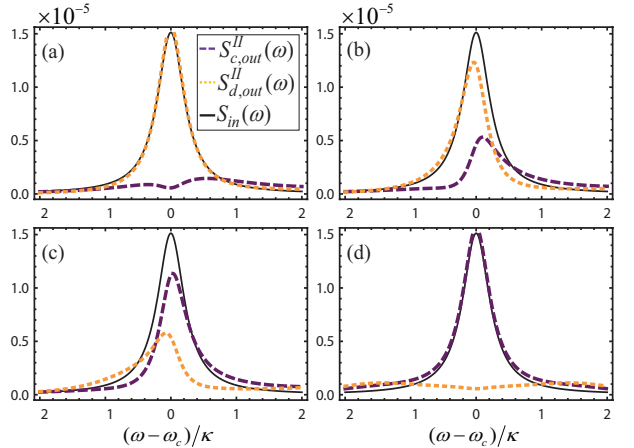


FIG. 5: (color online) The spectrum of the output fields  $S_{c,out}^w(\omega)$  (purple dashed lines),  $S_{d,out}^w(\omega)$  (orange dotted lines) and the input fields  $S_{in}(\omega)$  (black solid lines) for different  $\omega_d$ : (a)  $\omega_d/\omega_m = 0.8$ , (b)  $\omega_d/\omega_m = 0.85$ , (c)  $\omega_d/\omega_m = 0.9$ , (d)  $\omega_d/\omega_m = 1$ . The thermal phonon occupation number  $n_{th} = 0.05$ , and the other parameters are the same as in Fig. 4.

= 0, now the single-photon will be completely reflected through the cavity to the left output port. In this way, we can also achieve the routing of the single-photon.

Now we consider the effects of the quantum and thermal noises in this case. In Fig. 4(c)-(f), we plot the spectrums of the scattering probabilities  $L_3, \dots, L_6$ , respectively. We find that, in the range of the parameters we considered ( $\varepsilon_d/\omega_m = 2.56 \times 10^{-5}$ ), at  $\omega - \omega_c = 0$ ,  $L_3, \dots, L_6$  have the following order of magnitudes: when  $\omega_d = 0.8\omega_m$  or  $\omega_m$ ,  $L_3 \sim 10^{-5}$ ,  $L_4, L_5 \sim 10^{-8}$ , and  $L_6 \sim 10^{-12}$ . Comparing with the case of that there is no a weak coherent field, we can see that, now the vacuum fluctuations of the input fields  $\hat{c}_{in}(\omega)$  and  $\hat{d}_{in}(\omega)$  have been effectively suppressed, while the vacuum fluctuation of the input field  $\hat{b}_{in}(\omega)$  has been amplified. Moreover, now the system is working at the peak frequency of the single-photon, so the signal  $S_{in}(\omega_c)$  has order of magnitude  $10^{-5}$ . By comparing these order of magnitudes, we find that, the spectrum of the output fields can be reduced to

$$S_{c,out}^{II}(\omega) = L_1^c S_{in}(\omega) + L_3 n_{th}, \quad (23)$$

$$S_{d,out}^{II}(\omega) = L_1^d S_{in}(\omega) + L_3 n_{th}, \quad (24)$$

and we can see that, if the the thermal phonon occupation number  $n_{th} < 0.1$ , i.e., the mechanical resonator is cooled near its quantum ground state, the effects of the quantum and thermal noises on the single-photon can be neglected.

In Fig. 5, we plot the spectrum of the output fields  $S_{c,out}^{II}(\omega)$  and  $S_{d,out}^{II}(\omega)$  for different  $\omega_d$ . It can be seen

that, when  $\omega_d = 0.8\omega_m$ ,  $S_{d,out}^{II}(\omega) \approx S_{in}(\omega)$ ,  $S_{c,out}^{II}(\omega) \approx 0$  at  $\omega - \omega_c = 0$ . If we increase  $\omega_d$ ,  $S_{d,out}^{II}(\omega)$  will gradually decrease, and  $S_{c,out}^{II}(\omega_c)$  will gradually increase near  $\omega - \omega_c = 0$ . when  $\omega_d = \omega_m$ , we have  $S_{c,out}^{II}(\omega) \approx S_{in}(\omega)$ ,  $S_{d,out}^{II}(\omega) \approx 0$  at  $\omega - \omega_c = 0$ . So in this way, our system can act as a single-photon router.

## V. CONCLUSION

In summary, we have investigated the routing of a single-photon in a modulated cavity optomechanical system, in which the cavity is driven by a strong coupling field, the mechanical resonator (MR) is modulated by a weak coherent field, and the signal photon is made up of a sequence of pulses with exactly one photon per pulse. We demonstrated that, without the weak coherent field, the signal will be completely covered by the quantum and thermal noises, and the single-photon cannot be routed. With the existence of the weak coherent field, the single-photon can be routed at its peak frequency by changing the frequency of the weak coherent field.

## ACKNOWLEDGEMENTS

This work was supported by the National Natural Science Foundation of China (Nos. 11574092, 61775062, 61378012, 91121023); the National Basic Research Program of China (No. 2013CB921804); the Innovation Project of Graduate School of South China Normal University.

- 
- [1] S. E. Harris and Y. Yamamoto, Phys. Rev. Lett. **81**, 3611 (1998).
  - [2] M. Mücke, E. Figueroa, J. Bochmann, C. Hahn, K. Murr, S. Ritter, C. J. Villas-Boas, and G. Rempe, Nature (London) **465**, 755 (2010).
  - [3] P. Bermel, A. Rodriguez, S. G. Johnson, J. D. Joannopoulos, and M. Soljačić, Phys. Rev. A **74**, 043818 (2006);
  - [4] L. Zhou, Z. R. Gong, Y. X. Liu, C. P. Sun, and F. Nori, Phys. Rev. Lett. **101**, 100501 (2008);
  - [5] S. Sandlu, M. L. Povinelli, and S. Fan, Appl. Phys. Lett. **96**, 231108 (2010).
  - [6] J. Lu, L. Zhou, L. M. Kuang, and F. Nori, Phys. Rev. A **89**, 013805 (2014).
  - [7] J. Lu, Z. H. Wang, and L. Zhou, Opt. Express **23**, 22955 (2015).
  - [8] W. B. Yan, and H. Fan, Sci. Rep. **4**, 4820. (2014).
  - [9] G. Gautam, S. Kumar, S. Ghosh, and D. Kumar, J. Phys. B: At., Mol. Opt. Phys. **49**, 065502. (2016).
  - [10] C. H. Yan, Y. Li, H. Yuan, and L. F. Wei, Phys. Rev. A **97**, 023821 (2018).
  - [11] M. A. Hall, J. B. Altepeter, and P. Kumar, Phys. Rev. Lett. **106**, 053901 (2011).
  - [12] I. C. Hoi, C. M. Wilson, G. Johansson, T. Palomaki, B. Peropadre, and P. Delsing, Phys. Rev. Lett. **107**, 073601 (2011).
  - [13] L. Zhou, L. P. Yang, Y. Li, and C. P. Sun, Phys. Rev. Lett. **111**, 103604 (2013).
  - [14] G. S. Agarwal, and S. Huang, Phys. Rev. A **85**, 021801 (2012).
  - [15] D. Rugar and P. Grütter, Phys. Rev. Lett. **67**, 699 (1991).
  - [16] A. Szorkovszky, G. A. Brawley, A. C. Doherty, and W. P. Bowen, Phys. Rev. Lett. **110**, 184301 (2013).
  - [17] G. J. Milburn, Eur. Phys. J. Special Topics, **159**, 113 (2008).
  - [18] S. Basiri-Esfahani, C. R. Myers, J. Combes, and G. J. Milburn, New J. Phys. **18**, 063023 (2016).
  - [19] E. X. DeJesus and C. Kaufman, Phys. Rev. A **35**, 5288 (1987).
  - [20] D. Vitali, S. Gigan, A. Ferreira, H. R. Böhm, P. Tombesi, A. Guerreiro, V. Vedral, A. Zeilinger, and M. Aspelmeyer, Phys. Rev. Lett. **98**, 030405 (2007).
  - [21] R. Ghöbadi, A. R. Bahrapour, and C. Simon, Phys. Rev. A **84**, 033846 (2011).
  - [22] C. W. Gardiner and M. J. Collett, Phys. Rev. A **31**, 3761 (1985).
  - [23] J. M. Doherty, I. Wilson-Rae, and T. J. Kippenberg, Phys. Rev. Lett. **101**, 263602 (2008).
  - [24] S. Gröblacher, K. Hammerer, M. Vanner, and M. Aspelmeyer, Nature (London) **460**, 724 (2009).